Scientia Iranica (2025) **32**(6): 7127

Sharif University of Technology
Scientia Iranica
Transactions on Mechanical Engineering
https://scientiairanica.sharif.edu

An efficient biogas-base tri-generation of power, heating and cooling integrating inverted Brayton and ejector transcritical CO_2 cycles: Exergoeconomic evaluation

Ali Akbar Darabadi Zare [a], Farzad Mohammadkhani [b,*], Mortaza Yari [a,*]

a. Faculty of Mechanical Engineering, University of Tabriz, Tabriz, Iran.
b. Department of Mechanical Engineering, Engineering Faculty of Khoy, Urmia University of Technology, Urmia, Iran.

* Corresponding authors: f.mohammadkhani@uut.ac.ir (F. Mohammadkhani); myari@tabrizu.ac.ir (M. Yari)

Received 3 September 2022; received in revised form 4 June 2023; accepted 10 July 2024

Keywords

Gas turbine;
Inverted Brayton;
Transcritical carbon dioxide refrigeration;
Ejector expansion;
Exergoeconomics.

Abstract

In the present work, an efficient multigeneration system is proposed to meet diverse energy requirements such as power, heating, and cooling. The system consists of a biogas-fueled gas turbine cycle as the topping cycle, and a Brayton, an inverted Brayton, and also, a trans critical carbon dioxide refrigeration cycles with an ejector expansion as the bottoming cycles Using the ejector instead of compressor results in a reduction in the power consumption. Moreover, the required power of the refrigeration cycle can meet by the inverted Brayton cycle which eliminates the need for an external power source. The thermodynamic and exergoeconomic evaluations are done for the suggested system considering the energy and exergy efficiencies and total specific cost of the system as objective functions. Also, a parametric analysis is performed to specify the effects of decision variables on the system performance. The energy and exergy efficiencies and total cost rate of the system are determined as 79%, 44.4%, and 183.4 \$/h, respectively. These values demonstrate that the energy and exergy efficiencies of the proposed system have been improved by 48.9% and 54%, respectively, compared to the gas turbine cycle. Also, the cost of produced electricity is calculated to be 52.84 \$/MWh.

1. Introduction

In recent years, the growing trend of energy consumption has caused an energy crisis in the world. Therefore, energy and energy saving is one of the most serious issues in the world. Global concerns in addition to energy supply problems, include environmental problems such as ozone depletion, air pollution, acid rain, deforestation, and radioactive emissions. These problems must be considered simultaneously so that humanity can achieve a future with a definite energy with least environmental impact [1]. Pollution reduction and minimizing the fossil fuel consumption are possible through a strong focus on environmental sustainability. Cogeneration systems fueled by renewable fuels are some of the most suitable options to achieve this goal. One of these renewable fuels is biogas, which is produced from the anaerobic decomposition of biomass [2]. This method is best solution to dissolve this obstacle and get rid of wastes. In recent years, researchers have done more research on the Combined Cooling, Heat and Power (CCHP) system based on renewable energy and waste heat recovery to decrease the required energy and emission of pollutants. Recently, in industrialized countries, more than 50% of the heat from the combustion of fuel in the engine is wasted by the coolant and exhaust [3,4].

Darabadi Zareh et al. [2], analyzed exergy and exergoeconomic performance of a cogeneration system fueled by the blend of natural gas and biogas. They used municipal solid waste as the feedstock to the digestion. The results revealed that in the absence of biogas, the Heat Recovery Steam Generator (HRSG) and combustion chamber have the highest exergy destruction rate while it is

To cite this article:
A.A. Darabadi Zare, F. Mohammadkhani, M. Yari "An efficient biogas-base tri-generation of power, heating and cooling integrating inverted Brayton and ejector transcritical CO_2 cycles: Exergoeconomic evaluation", *Scientia Iranica* (2025) **32**(6): 7127 https://doi.org/10.24200/sci.2024.61064.7127

highest for the anaerobic digester and combustion chamber in the absence of NG. Moreover, the exergy efficiency of the cycle in the case of pure biogas and pure natural gas was 46.94% and 50.64%, respectively.

Yang et al. [5], studied thermo-economic evaluation of multiple production system of cooling, power and heating by gasification of biomass fuel. Sensitivity analysis showed that the most sensitive factor for the cost of the manufactured products is the cost of biomass. Also, the unit exergetic cost of electricity was estimated as 4.445, 4.447 and 4.447 for the cold season, warm season, and transition season, respectively. Uris et al. [6]. assessed and compared the performance of the CHP and CCHP systems with biomass fuel in Spain. The Organic Rankine Cycle (ORC) was used in both systems. The results showed that the emission of carbon dioxide in the CHP system is more than the CCHP system.

Leonzio [7], proposed a novel cogeneration system which uses biogas as a renewable fuel. They burned 3280 kW biogas to produce 925 kW electricity and 1875 kW heating.

Shu et al. [3], introduced CTRC (CO_2 Transcritical Rankine Cycle) including the regenerator and preheater for recovering waste heat in exhaust gas of an engine. The results show the considerable advantage of extremely recycling the engine coolant and exhaust gas. The Preheater and Regenerator upgrades the exergy efficiency and energy efficiency of the CTRC (PR-CTRC), with increases of 227% and 184%, respectively. Mohammadi and Powell [8] analyzed new multi-generation systems based on carbon dioxide refrigeration cycles. The systems are examined considering 1 MW capacity and evaporator temperatures of -35°C to -45°C. Carbon dioxide has attracted a lot of attention due to its many advantages as a working fluid in various cycles. First of all, CO_2 has no restriction on the temperature of thermal decomposition. Secondly, heat can be transferred directly from the exhaust gases to carbon dioxide, and due to the transcritical state of the carbon dioxide in the evaporator, a better temperature matching can be achieved. Thirdly, carbon dioxide is non-flammable and environmental friendly [9].

Yari [10], assessed the performance of a two-stage ejector trans critical refrigeration CO_2 cycle, which uses an intercooler and an internal heat exchanger to increase the system efficiency. The results confirm that the Coefficient of Performance (COP) and exergy efficiency for the novel two-stage ejector expansion system are on average 12.5–21% more than those for the conventional two-stage system. Domanski reported that the ejector efficiency is more important feature in the performance coefficient of the ejector expansion refrigeration cycle. The amount of COP betterment depends on the refrigerant's thermodynamic properties and it is different from system to system [11,12]. The ejector is a low-cost, simple and easy-to-maintain device with high capability for suction, mixing of flows and compression. Thus, ejector has high potential in exergy and energy exploitation. Nevertheless, the CCHP system can utilize the gas turbine and ejector-refrigeration cycle for multiple production of power, heat and cold.

Dai et al. [13], introduced a combined power and refrigeration cycle with carbon dioxide refrigerant which is driven by the renewable energy source or flue gas of the engine. The results of parametric study showed that condenser temperature, evaporator temperature, and turbine inlet pressure had the greatest effect on the system performance. Also, it is concluded that the steam heat exchangers, ejectors and turbines are the most destructive components from the exergy viewpoint.

Gholizadeh et al. [14], proposed a triple generation system of cooling, fresh water and electricity by utilizing the geothermal heat source. One of the most important advantages of this proposed system was the ability to produce cooling at two different temperatures by utilizing the two ejector refrigeration cycles. The optimization results showed that the cooling effect, exergy efficiency and power generation were increased to 87%, 46.3% and 77%. Song et al. [15], studied the exergy and economic evaluation of the hybrid system. This system was a combination of supercritical carbon dioxide and ORCs. The results displayed that the total power produced is 2940 kW.

Yari [16], performed thermodynamic analysis on the ejector-vapor compression refrigeration cycle. Based on the results, COP and exergy efficiency of the novel system are about 16% more than the vapor compression cycle. Tashtoush et al. [17], studied a novel trans critical refrigeration cycle from the thermodynamic and thermoeconomic viewpoints. The results showed that total cost of the final product and overall exergy destruction rate are 6% and 22.25% less than the conventional ejector refrigeration cycle, respectively.

Wang et al. [18], simulated the cogeneration system of power and cooling from the energy, exergy and exergoeconomic viewpoints by employing of low-temperature heat sources. The results showed that the ejector has the highest irreversibility among the system components. Also, this proposed system can provide 18.52 kW of power and 23.89 kW of cooling and the efficiencies of the first and second laws of thermodynamic were 21.7% and 52.22%, respectively. In another study, Karim et al. [19], investigated and optimized the polygeneration system of cooling, power and heating with solar energy. The system was analyzed from thermodynamic and thermoeconomic perspectives. The results showed that the total cost rate and the exergy efficiency at the optimal point are 0.4835 $/h and 10.06% respectively.

Sahu et al. [20], studied transcritical carbon dioxide refrigeration and combined refrigeration-power systems. They also did a sensitivity analysis on the COP and the second-law efficiency. The results revealed that the COP rises with turbine inlet temperature. Also, the exergy efficiency has a maximum value with the turbine inlet temperature. Cao et al. [21], proposed new systems with biogas fuel for power and cooling, and analyzed and optimized the systems in terms of energy and exergy. The results showed that the steam generator has the highest irreversibility rate in the downstream cycle and the combustion chamber has the highest irreversibility rate in the gas turbine cycle. Also, the energy and exergy efficiencies of the system improved after optimization and reached 57.11% and 36.68%, respectively.

Chen et al. [22], introduced a power generation system combined with a carbon dioxide Brayton cycle and a carbon-dioxide air conditioning for vehicles engine utilizing waste energy of the exhaust gas. The proposed system is not attractive due to the high consumption of the compressor as most of the produced power will be used to provide part of the required power by the compressor in the refrigeration part of the system. Wang et al. [23], proposed transcritical carbon dioxide cycle for trigeneration of power, heating, and cooling, operating by solar energy. In this proposed system, the total net power is zero or close to zero in the different operating conditions, so input power is required for cycle operation.

Sinha et al. [24] analyzed the energy and exergy of power generation systems. The results showed that by adding heat recovery and fuel cell to the system, the performance of the system increases.

Kumar et al. [25] studied the thermodynamic analysis of the integrated system of gas turbine cycle with solid oxide fuel cell and ORC. By a conducting a parametric study, the results showed that the maximum energy and exergy efficiencies of the proposed system are 47.34% and 56.85%, respectively.

Mohammadi et al. [26] studied the thermodynamic analysis of multiple generation system of power, cooling and heating. The results showed that gas turbine inlet temperature and pressure ratio are the most effective influencing parameters.

Considering the above discussion, it could be deduced that inventing a trigeneration system of the power, and cooling, heating with high efficiency driven by renewable fuel as the input energy, and also, the use of safe and environmentally friendly refrigerant as a coolant in the refrigeration systems is necessary. Accordingly, in the present work, to increase the thermal and exergy efficiencies, a new arrangement based on ejector CO_2 transcritical cycle has been proposed. In this work, by using the ejector instead of the compressor, the power consumption is reduced. Moreover, by applying the inverted Brayton cycle in the refrigeration cycle, the generated power improves the system efficiency, as well as the required power for the refrigeration system, as the sub-cycle does not need to be supplied from another resource. Biogas is suggested as a fuel owing to its many benefits illustrated in our previous works [2,27]. The proposed hybrid system with carbon dioxide working fluid has been analyzed in terms of thermodynamics and exergoeconomics using a developed simulation model in Engineering Equation Solver (EES). This system combines a Gas turbine, a Brayton, an inverted Brayton and a refrigeration cycle with ejector expansion. Also, to identify the influences of the various thermodynamic parameters on the system performance, a parametric assessment has been accomplished. Briefly, the novelties and main objectives of the work can be written as:

- Proposing a novel efficient multigeneration configuration to recover the waste heat of a biogas-fueled gas turbine combining a gas turbine, a Brayton, an inverted Brayton, and a refrigeration cycles with ejector expansion;
- Employing an ejector instead of the compressor to reduce the power requirement;
- Using an inverted Brayton cycle to meet the required power of the refrigeration subsystem and eliminate the need for the external power source;
- Evaluating the proposed system in terms of thermodynamics and exergoeconomics;
- Performing a parametric study to identify the effects of decision variables on the thermodynamic and exergoeconomic parameters of the system.

2. System description

The proposed CCHP system is shown in Figure 1, that includes a biogas fueled gas turbine as the topping cycle while the bottoming cycle consists of a Brayton, an inverted Brayton and an ejector-expansion transcritical CO_2 refrigeration cycles followed by a single-pressure HRSG. The bottoming cycle utilizes the waste heat of the gas turbine exhaust from the topping cycle through a gas heater. According to Figure 1, air enters to the air compressor at the atmospheric pressure and temperature (1) and is pressurized to the operating pressure of the gas turbine (2). The pressurized air enters to the Air Pre-Heater (APH) until its temperature reaches to 700 K (3). Then, it is burned with the biogas in the combustion chamber. Flue gases leave the combustion chamber at 1250 K and enter the gas turbine (4) where 1 MW of power is generated. After passing the turbine, flue gas enters the preheater (5), and then, to use the dissipated heat and also supply the supercritical cycle of carbon dioxide, it enters into the gas heater to transfer heat (6). The hot gasses leaving the gas heater enter the HRSG (7). From the other side, water at the temperature of 25°C and the pressure of 3500 kPa enters the HRSG and comes out of it as saturated steam. Sub-critical carbon dioxide (22) is sent to the compressor and is compressed to a supercritical state (23). SCO_2 enters the gas heater to reach the desired temperature (8). After leaving the gas heater, the high-temperature supercritical CO_2 enters the High Pressure (HP) and Low Pressure (LP) turbines and expands to a lower pressure to generate power (9,10). The output carbon dioxide from the LP-turbine enters the heater to provide district heating (11). After leaving the heater, carbon dioxide enters the compressor and reaches the desired pressure (12), and then loses heat in the gas cooler (13). Then, carbon dioxide enters the ejector to entrain the secondary flow (18) from the evaporator. The carbon dioxide stream enters to the separator (14) after leaving the ejector to separate the saturated vapor and saturated liquid. Saturated liquid enters the evaporator

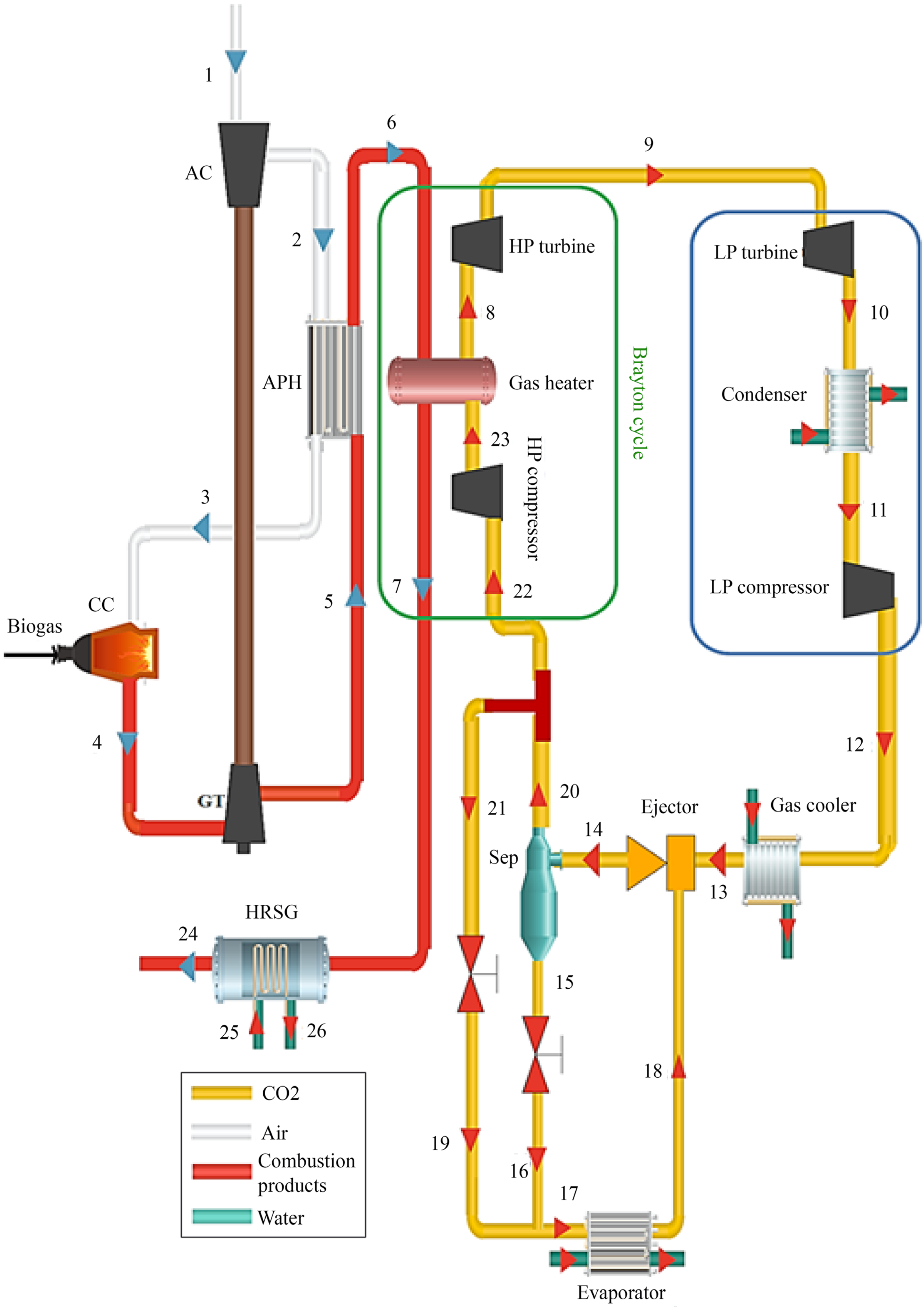

Figure 1. Schematic diagram of the CCHP system integrating inverted Brayton cycle and ejector transcritical CO_2 driven by biogas combustion.

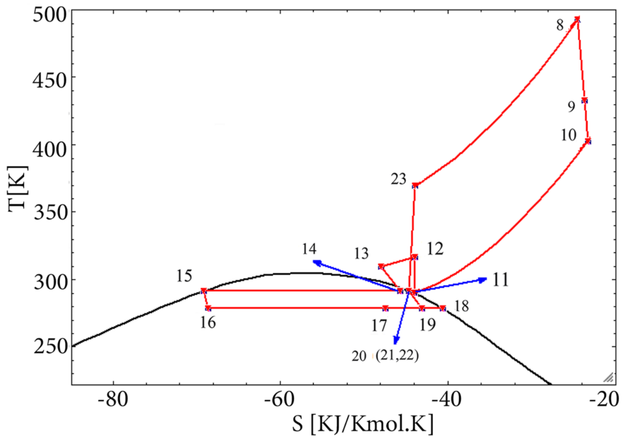

Figure 2. T-S diagram of the CCHP subsystem with transcritical CO_2.

after crossing by the throttle valve (15), and also, a portion of the carbon dioxide saturated vapor is returned to the evaporator through the throttle valve (21). It is worth noting that in Figure 2 shows the T-s diagram for the proposed CCHP subsystem.

3. Modeling

Energy and exergy and exergoeconomic modeling of the proposed CCHP system is done using the developed simulation code in EES. More attention is paid to the combustion chamber and ejector, since they are important components of the systems. For this reason, modeling of the combustion chamber and ejector are described in Subsections 3.5 and 3.4, respectively.

3.1. *Energy analysis*

In this study, with assuming steady state condition and neglecting the changes of potential and kinetic energies mass balance and the first law of thermodynamics equations are written as follows [2,27]:

$$\sum_{in} \dot{m} = \sum_{out} \dot{m}, \tag{1}$$

$$\sum \dot{Q} + \sum_{in} \dot{m}h = \sum \dot{W} + \sum_{out} \dot{m}h. \tag{2}$$

3.2. *Exergy analysis*

The exergy equation for a control volume is defined as below [28]:

$$\sum_{in} \dot{E}_i = \sum_{out} \dot{E}_j + \dot{I}, \tag{3}$$

where, $\dot{E}_i$ and $\dot{E}_j$ are the input and output exergy rates of the component, respectively. Also, $\dot{I}$ is the exergy destruction rate of the component.

Exergy is divided into the chemical and thermo-mechanical parts. In the absence of the surface tension, magnetic, electrical and nuclear effects, the total kinetic, potential and physical exergies are defined as thermo-mechanical exergy.

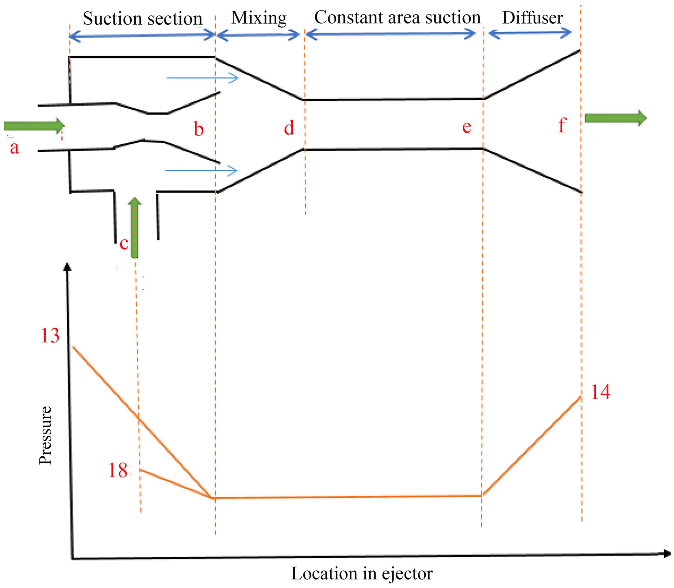

Figure 3. The schematic of an ejector.

$$E_{tot} = E_{th} + E_{ch}, \tag{4}$$
$$E_{th} = E_{ph} + E_{pt} + E_{kn}. \tag{5}$$

The potential and kinetic exergies are negligible, so thermo-mechanical exergy is defined as [29]:

$$\dot{E}_{th} = \dot{E}_{ph} = \dot{m}\big(h - h_0 - T_0(s - s_0)\big), \tag{6}$$

here, s, T, and h are specific entropy, temperature and specific enthalpy, respectively. Chemical exergy is defined as [29]:

$$\bar{E}^{CH} = \sum x_i\, \bar{e}^{CH} + \bar{R}T_0 \sum x_i \ln x_i, \tag{7}$$

which $\bar{R}$ and x_i are the universal gas constant and the mole fraction of the ith gas, respectively.

The assumed values for the simulation of the proposed CCHP system are given in Table A.1 in Appendix A. To thermodynamic modeling, the made assumptions in this study are as follows:

- The compressors and turbines isentropic efficiencies are 86% [1];
- The pressure drops in the APH and the combustion chamber are 5% and 4%, respectively;
- All processes are steady state ($\frac{d}{dt} = 0$) [29];
- The streams through the throttle valves are constant enthalpy;
- The exiting flow from the evaporator is saturated vapor.

3.3. *Ejector*

The structure of the ejector that is one of the most important components of the CCHP system consists of four parts: suction, mixing, constant-area and diffuser sections as seen in Figure 3. The gas cooler output stream as a high-pressure motive stream enters the ejector which has an insignificant velocity and entrains secondary stream from evaporator, which has less pressure than the primary fluid. The entrainment ratio is one of the important characteristics of ejectors which is written as the ratio of the secondary to primary mass flow rates. Then the streams are blended in the mixing section. If the mixed fluid is supersonic, a shock wave will occur in the diffuser inlet, that causes the refrigerant velocity to reach from the supersonic to the subsonic state, and consequently, pressure will be increased by the diffuser to separator pressure. It is worth noting that the ejector can be assortment into two kinds based on the situation of the nozzle: constant-pressure mixing and constant-area mixing [23]. It is assumed in this study that the mixing of ejector takes place at the constant pressure. The details of the mathematical model (energy, momentum and mass) for the ejector can be written as below. In the nozzle section, the energy equation for the primary current is defined as follows:

$$h_{pr,n1}+\frac{v_{pr,n1}^2}{2}=h_{pr,n2}+\frac{v_{pr,n2}^2}{2}. \quad (8)$$

In comparison with the exit velocity of primary stream $h_{pr,n2}$, the inlet velocity of primary stream $h_{pr,n1}$ could be insignificant.

$$v_{pr,n2}=\sqrt{2\times(h_{pr,n1}-h_{pr,n2})}. \quad (9)$$

Nozzle efficiency is defined as follows:

$$\eta_{nazzle}=\frac{h_{pr,n1}-h_{pr,n2}}{h_{pr,n1}-h_{pr,n2,s}}. \quad (10)$$

Hence, by combining Eqs. (9) and (10), Eq. (11) is obtained:

$$v_{pr,n2}=\sqrt{2\times\eta_{nazzle}(h_{pr,n1}-h_{pr,n2,s})}. \quad (11)$$

The entrainment ratio of the ejector can be defined as follows:

$$\mu=\frac{\dot{m}_{Se}}{\dot{m}_{pr}}. \quad (12)$$

Also, the energy equation for the secondly stream is expressed as:

$$h_{se,n1}+\frac{v_{se,n1}^2}{2}=h_{se,n2}+\frac{v_{se,n2}^2}{2}. \quad (13)$$

In comparison with the exit velocity of secondly stream $h_{se,n2}$, the inlet velocity of secondly stream $h_{se,n1}$ could be insignificant.

$$v_{se,n2}=\sqrt{2\times(h_{se,n1}-h_{se,n2})}, \quad (14)$$

$$\eta_{nazzle}=\frac{h_{se,n1}-h_{se,n2}}{h_{se,n1}-h_{se,n2,s}}. \quad (15)$$

By combining Eqs. (14) and (15), Eq. (16) is obtained:

$$v_{se,n2}=\sqrt{2\times\eta_{nazzle}(h_{se,n1}-h_{se,n2,s})}\,. \quad (16)$$

As well as in the mixing section, the momentum conservation equation can be written as below:

$$m_{pr,n2}\times v_{pr,n2}+m_{se,n2}\times v_{se,n2} = (m_{pr,n2}+m_{se,n2})\times v_{mix}. \quad (17)$$

Hence, by combining Eqs. (12) and (17), one can write:

$$v_{mix,s}=\frac{v_{pr,n2}+\mu\times v_{se,n2}}{1+\mu}. \quad (18)$$

The mixing efficiency is given as:

$$\eta_m=\frac{v_{mix,m}^2}{v_{mix,s}^2}. \quad (19)$$

$$v_{mix,m}=\sqrt{\eta_m}\times\frac{v_{pr,n2}+\mu\times v_{se,n2}}{1+\mu}. \quad (20)$$

The energy equation for the mixing section is defined as follows:

$$\dot{m}_{pr}\left(h_{pr,n2}+\frac{v_{pr,n2}^2}{2}\right)+\dot{m}_{se}\left(h_{se,n2}+\frac{v_{se,n2}^2}{2}\right) = (\dot{m}_{pr}+\dot{m}_{se})\times\left(h_{mix}+\frac{v_{mix,m}^2}{2}\right). \quad (21)$$

By combining Eqs. (12) and (21), Eq. (22) is obtained:

$$h_{mix}=\frac{1}{1+\mu}\times(h_{pr,n2}+\frac{v_{pr,n2}^2}{2})+\frac{\mu}{1+\mu} \times(h_{se,n2}+\frac{v_{se,n2}^2}{2})-\frac{v_{mix,m}^2}{2}\,. \quad (22)$$

Also, the output enthalpy and temperature of diffuser section is calculated as (by developing a simulation code in EES):

$$h_{di,s}=f(S_{di,s},P_{14}). \quad (23)$$

Diffuser efficiency is defined as follows:

$$\eta_{dif}=\frac{h_{di,s}-h_{mix}}{h_{di,a}-h_{mix}}. \quad (24)$$

From Relation (24), relation (25) is obtained:

$$h_{di,a}=h_{mix}+\frac{h_{di,s}-h_{mix}}{\eta_{dif}}. \quad (25)$$

Finally, the ejector outlet temperature is calculated as (by writing code in EES program):

$$T_{14}=f(h_{dia},P_{14}). \quad (26)$$

3.4. Combustion chamber

It is considered that the combustion process happens in the combustion chamber with the excess air. As example for one mole of fuel, reaction equation is written as follows:

$$\begin{aligned}&0.6CH_4+0.4CO_2+n_3(0.2059O_2+0.7748N_2\\&+0.0003CO_2+0.019H_2O)®(1+0.0003n_3)CO_2\\&+(1.2+0.019n_3)H_2O+0.7748n_3N_2+(0.2059n_3\text{ -}1.2)O_2\end{aligned} \quad (27)$$

where n_3 is the air mole numbers of combustion chamber. As mentioned above, the equation of the first law for the combustion chamber is written as follows [2,30]:

$$\dot{Q}-\dot{W}=\dot{n}*\bar{h}_{pr}-\dot{n}_{react}*\bar{h}_{react} \quad (28)$$

here, heat transfer to the environment and the enthalpy of the products are calculated as follows:

$$\dot{Q}=0.02*\dot{n}_f*\overline{LHV}_F \quad (29)$$

$$\bar{h}_{pr}=X_{CO2}\bar{h}_{CO2}+X_{H2O}\bar{h}_{H2O}+X_{N2}\bar{h}_{N_2}+X_{O2}\bar{h}_{O2} \quad (30)$$

where, X_{CO_2}, X_{H_2O}, X_{N_2}, and X_{O_2} are the molar fraction of combustion products components.

$$X_{CO_2} = \frac{1+0.0003n_3}{1+n_3},\ X_{H2O} = \frac{1.2+0.019n_3}{1+n_3}\ ,$$

$$X_{N2} = \frac{0.7748n_3}{1+n_3}, \qquad X_{O2} = \frac{0.2059n_3-1.2}{1+n_3}\ .$$

3.5. Exergoeconomic analysis

Exergoeconomics is a powerful technique for evaluation and optimization of energy systems which is the combination of economic principles and the second law of thermodynamics. This method provides useful information that exergy or economic cannot handle separately. In this field, many approaches have been presented, including the methods of average cost approach, the exergy cost theory and the Specific Exergy Costing (SPECO). In this study, exergoeconomic analysis has been employed based on SPECO method due to the easy procedure and lower calculation time. To start the analysis in this method, in the first stage, all input and output flows are identified in the system boundary and are introduced as product or fuel. Then, the cost balance is expanded for components of the system as:

$$\sum_j \dot{C}_{j,m} + \dot{C}_{w,m} = \dot{C}_{q,m} + \sum_i \dot{C}_{i,m} + \dot{Z}_m, \tag{31}$$

here, the subscripts i and j indicate input and output streams, respectively. $\dot{Z}$ expresses sum of the cost rate of Capital Investment (CI) and cost rate interdependent with Operation and Maintenance (OM), and $\dot{C}$ is the cost rate. Also, $\dot{C}_{q,k}$ and $\dot{C}_{w,k}$ represent the cost rate associated with heat transfer and work, respectively, and are written as follows:

$$\dot{C}_i = c_i\dot{E}_i, \tag{32}$$

$$\dot{C}_j = c_j\dot{E}_j, \tag{33}$$

$$\dot{C}_q = c_q\dot{E}_q, \tag{34}$$

$$\dot{C}_W = c_W\dot{E}_W, \tag{35}$$

$$\dot{Z}_m = \dot{Z}^{cl}{}_m + \dot{Z}^{om}{}_m = CRF \times \frac{\phi_r}{N} \times PEC_m, \tag{36}$$

where, N indicates the annual operating hours, ϕ_r and PEC_k are the maintenance factor and the components' purchased cost in US dollar, respectively. Also, CRF depends on Beneficial Life (BL) and interest rate (i) and it is defined as:

$$CRF = \frac{i \times (1+i)^{BL}}{(1+i)^{BL} - 1}, \tag{37}$$

Which CRF is Capital Recovery Factor. In this study, i and BL are supposed to be 0.12 and 10 years, respectively. Also, the PEC of the components is given in Table A.2 in Appendix A.

In Eq. (29), auxiliary equations are needed as the number of unknown flow cost equations is more than the number of cost balance equations. Whenever the number of output exergy currents of a component is more than one ($k > 1$), the number of ($k - 1$) auxiliary equations will be needed. To develop the auxiliary equations, the P and F principles can be utilized. Using this method, a set of linear equations $\left([\dot{E}_k] \times [c_k] = [\dot{Z}_k]\right)$ is written for components of the system. Thus, the cost rate of all streams is obtained. Here, $[\dot{Z}_k]$ and $[\dot{E}_k]$ are obtained by Eq. (34) and exergy analysis, respectively, and so, $[c_k]$ which is the matrix of the specific cost can be appraised.

4. Performance parameters

To appraise the proficiency of a CCHP system, some indicators are determined. The thermal and exergy efficiencies of the CCHP system are defined as below [2]:

$$\eta_{th} = \frac{\dot{W}_{GT} + \dot{W}_{T1} + \dot{W}_{re} - \dot{W}_{C1} + \dot{Q}_{HRSG} + \dot{Q}_{Eva} + \dot{Q}_{Heater}}{\dot{m}_{bio} LHV_{bio}}, \tag{38}$$

$$\varepsilon = \frac{\dot{W}_{GT} + \dot{W}_{BC} + \dot{W}_{IBC} + \dot{E}_{26} - \dot{E}_{25} + \dot{E}_{eva} + \dot{Q}_{Heat} \times \left(1 - \frac{T_0}{T_{Heat}}\right)}{\dot{E}_1 + \dot{E}_{bio}}. \tag{39}$$

The $\dot{W}_{GT}$, $\dot{W}_{IBC}$ are the production power of the gas turbine cycle, inverted Brayton cycle, respectively, and they are defined as:

$$\dot{W}_{GT} = \dot{W}_T - \dot{W}_C, \tag{40}$$

$$\dot{W}_{IBC} = \dot{W}_{T,re} - \dot{W}_{C,re}. \tag{41}$$

$\dot{E}_{eva}$ is the exergy associated with the refrigeration output, which is calculated as follows:

$$\dot{E}_{eva} = \dot{m}_{eva} \times ((h_{eva,in} - h_{eva,out}) - T_0 \times (S_{eva,in} - S_{eva,out}). \tag{42}$$

And the total cost rate of the system, $\dot{C}_{system}$, is defined as:

$$\dot{C}_{system} = \dot{C}_F + \sum_i \dot{Z}_i + \sum_i \dot{C}_{D,i} + \dot{C}_L. \tag{43}$$

Which $\dot{C}_{D,i}$ is the exergy destruction cost rate. The average costs per the exergy unit are described as:

$$c_{p,k} = \frac{\dot{C}_{p,k}}{\dot{E}_{p,k}}, \tag{44}$$

$$c_{f,k} = \frac{\dot{C}_{f,k}}{\dot{E}_{f,k}}, \tag{45}$$

$$c_{D,k} = \frac{\dot{C}_{D,k}}{\dot{E}_{D,k}}. \tag{46}$$

Relative cost difference (r_k) and also exergoeconomic factor (f_k) are defined as Eqs. (45) and (46), respectively [27]:

$$r_k = \frac{c_{p,k} - c_{f,k}}{c_{f,k}}, \tag{47}$$

$$f_k = \frac{\dot{Z}_k}{\dot{Z}_k + \dot{C}_{D,k} + \dot{C}_{l,k}}. \tag{48}$$

5. Results and discussion

A simulation code is developed using EES to run the set of equations derived from the thermoeconomic modeling of each component. Figure 4 shows the solving methodology flowchart.

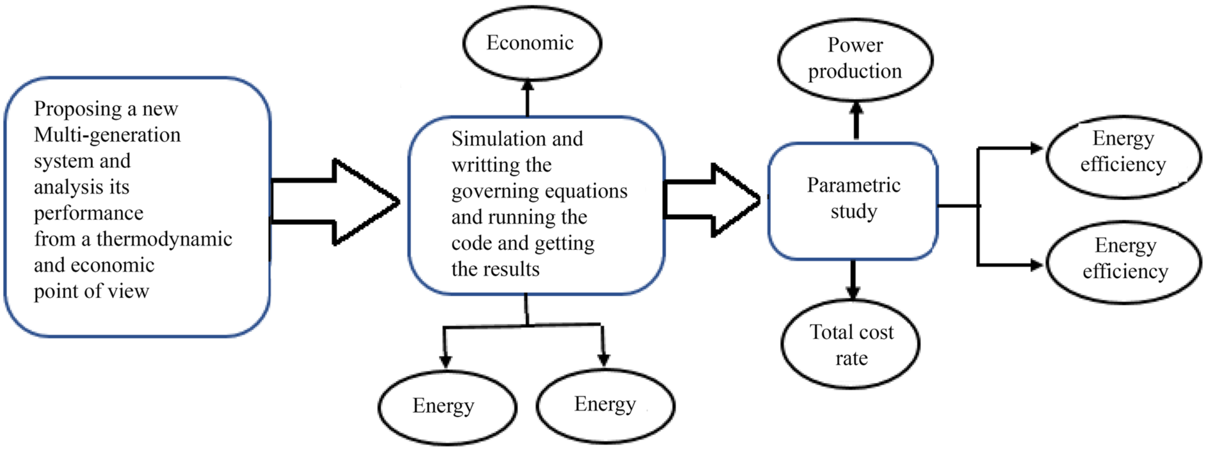

Figure 4. Solving methodology flowchart.

Table 1. Comparison of performance characteristics of gas turbine cycle in the present study and Refs. [21,30].

System performance characteristics	References	Present work
Gas temperature at turbine outlet (K)	817	820
Air temperature at compressor outlet (K)	596	593.9
Fuel to air ratio, λ	0.04341	0.04342
Air preheater outlet temperature (K)	723.7	724.2
Compressor power (kW)	1439	1404
Turbine power (kW)	2439	2404
Energy efficiency (%)	32.6	31.5
Exergy efficiency (%)	30.91	29.8

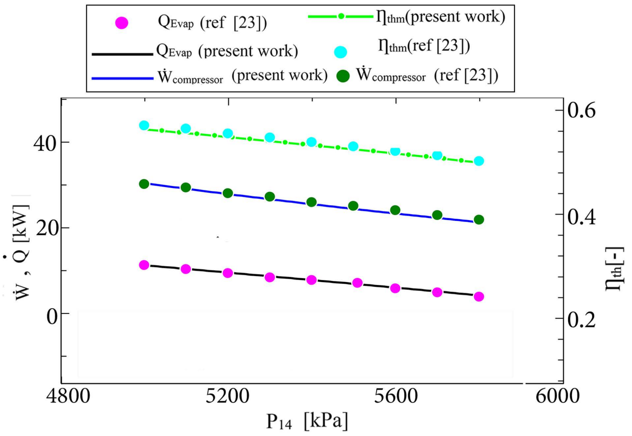

Figure 5. Comparison of compressor power, turbine power, first law efficiency and cooling effect for the present work and Wang et al. [23] by increasing the ejector back pressure.

To ensure the accuracy of the simulation, the results are compared with references [23,30]. The comparison for the gas turbine and transcritical CO_2 cycle are given in Table 1 and Figure 5, respectively, which shows a good agreement. The maximum relative difference between the results is about 2%. The schematic figure of Wang et al. [23] is shown in Figure 6.

5.1. *Energy and exergy analysis results*

In this section, the achieved results from energy, exergy, and exergoeconomic simulation and as well as the design parameters effects on the system performance are reported. Based on the described analysis in the previous section, a simulation program was developed in EES for the integration of a gas turbine cycle with a production capacity of 1000 kW, a Brayton cycle, an inverted Brayton cycle and a transcritical carbon dioxide refrigeration system with ejector. The thermodynamic properties of each stream for the CCHP system are given in Table A.3 in Appendix A. Also, Figure 7(a) and (b) show the exergy destruction contribution of each component of topping and bottoming cycles. In the topping cycle, the combustor and in the bottoming cycle, the ejector have the highest irreversibility due to the combustion and mixing of fluids, respectively. By applying the inverted Brayton cycle, the total power of the ejector refrigeration cycle will be positive, and the best possible amount of back pressure of the inverted Brayton turbine (LP turbine) will be 5300 kPa, resulting in a power production of 5 kW. Also, the values demonstrate that the energy and exergy efficiencies will improve by 48.9% and 54%, respectively, compared to the gas turbine cycle, as well as energy and exergy efficiencies of the proposed system will increase by 49.0% and 57%, respectively, compared to the basic cycle [23]. Table 2 shows the evaluation criteria of the proposed system from the thermodynamic viewpoint.

5.2. *Exergoeconomic analysis results*

The exergoeconomic results for the CCHP system are listed in Table 3. As can be seen from the results, the HRSG and combustion chamber have the maximum amount of $\dot{Z} + \dot{C}_D + \dot{C}_L$ among all the components. Thus, these components are the most important components in terms of thermo-economics.

Also, the heater and gas heater have the highest amount of relative cost difference, which shows the sharp increase in the product cost of these components. f_k which is the correlation between the exergy destruction and CI cost rates. Lower values of this parameter in the ejector and combustion chamber demonstrate that these are components with a higher cost rate associated with exergy destruction. Thus, exergy destruction

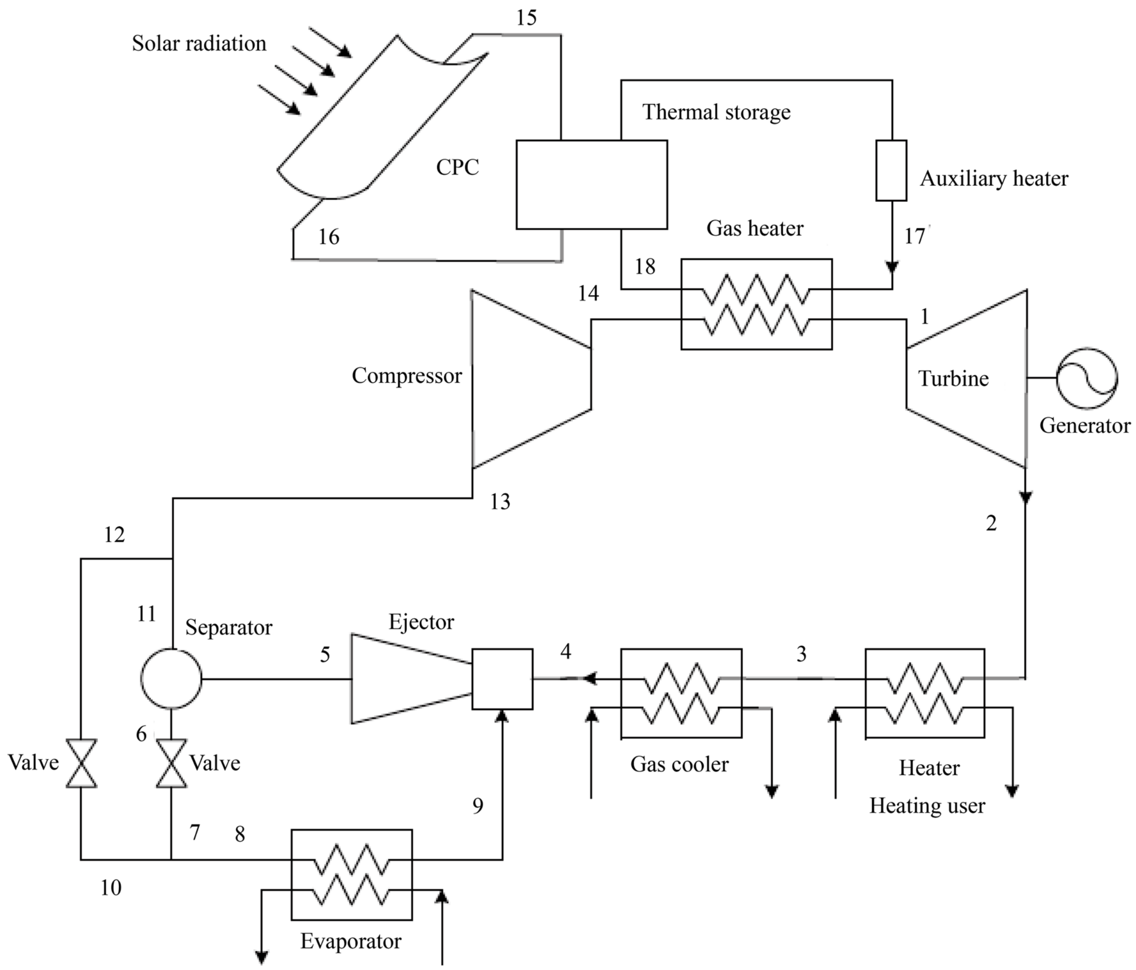

Figure 6. Schematic diagram of Wang et al. [23].

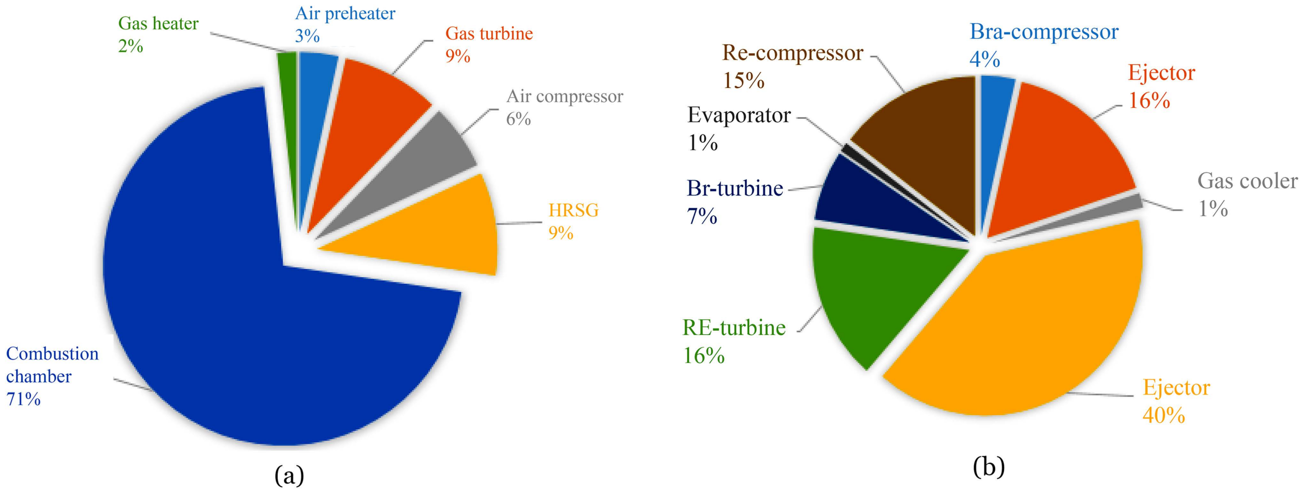

Figure 7. Exergy destruction contribution of components of (a) the topping cycle and (b) the refrigeration system.

Table 2. Results of system evaluation parameters.

Parameter (unit)	Value
Energy efficiency (%)	78.36
Exergy efficiency (%)	62.96
Refrigeration output (kW)	7.122
Heat recovered in the steam generator (kW)	1430
Inverted Brayton cycle output power (kW)	5

Table 3. Exergoeconomic analysis results of the components.

Components	c_f (\$/GJ)	c_p(\$/GJ)	$\dot{C}_D$ (\$/h)	$\dot{C}_L$(\$/h)	$\dot{Z}$ (\$/h)	$\dot{Z}+\dot{C}_D$ (\$/h)	r (%)	f (%)
LP-compressor	83.01	92.04	0.2	-	0.0093	0.21	10.87	4.44
Heater	62.91	314.9	1.72	-	0.1412	1.86	400.5	7.59
HP- compressor	81.23	93.15	0.815	-	0.049	0.86	14.67	5.67
LP- turbine	62.91	83.01	0.306	-	0.575	0.88	31.95	65.26
HP- turbine	62.91	81.23	0.684	-	0.943	1.63	29.12	57.95
Combustion chamber	10.25	13.55	44.43	-	0.192	44.62	32.19	0.43
HRSG	13.55	19.71	7.63	8.3	3.503	11.13	45.46	18
Air preheater	13.55	20.42	2.87	-	3.431	6.301	50.70	54.45
Air compressor	14.68	17.05	5.28	-	5.84	11.12	16.14	52.51
Gas turbine	13.55	14.68	7.27	-	2.518	9.78	8.33	25.74
Ejector	65.69	67.07	0.74	-	-	0.74	2.1	-
Gas cooler	64.48	250	1.43	-	0.233	1.67	287	14
Evaporator	70.17	113.9	0.045	-	0.007	0.052	62.32	12.79
Gas heater	13.55	26.92	1.44	-	0.018	1.46	98.67	1.20

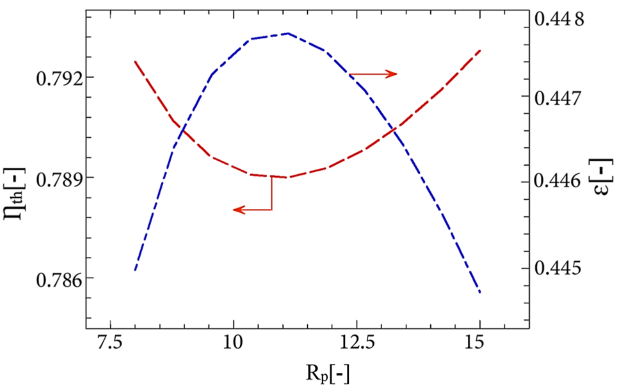

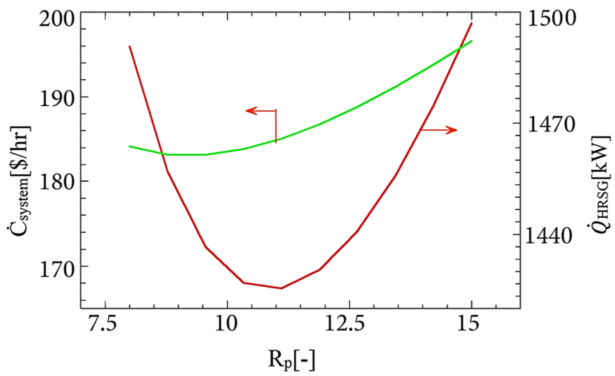

Figure 8. Effects of air compressor pressure ratio on the (a) energy and exergy efficiencies and (b) heat generated in the HRSG and the total cost rate of the system.

cost rate should be decreased to enhance exergoeconomic performance. Moreover, the higher amount of the exergoeconomic factor in the system components shows that the capital cost rate is superior to the exergy destruction cost rate. According to Table 3, the exergoeconomic factor of the gas turbine of inverted Brayton cycle has a maximum value among the components.

Based on the obtained results, total cost rate of the system and cost of produced electricity are 183 \$/h and 52.84 \$/MWh, respectively.

5.3. Parametric study

The selected parameters for the parametric study were air compressor pressure ratio, ejector back pressure, turbine inlet temperature, APH outlet temperature, HP turbine back pressure, ejector inlet temperature, HP-turbine inlet temperature and back pressure of the inverted Brayton turbine (LP turbine). To evaluate the effect of every parameter, the other parameters were kept fixed.

Figure 8(a) and (b) depict the influences of the air compressor pressure ratio on the system performance parameters. Because of the net power of gas turbine cycle is constant, the compressor input power and the gas turbine produced power rise by increasing this parameter. Thus, air flow rate first reduces and then increases. The enthalpy of the outlet and inlet streams of the combustion chamber are getting fixed. Thus, the biogas consumption first decreases and then increases. Thus, exergy and energy input to the system, and also, water stream and heat recovery of HRSG have minimum values with the air compressor pressure ratio. These trends will lead a minimum value for the energy efficiency of the system. Moreover, increasing pressure ratio, reduces the total cost rate of the system because of reduction in the fuel mass flow rate. However, for the pressure ratios greater than 10, by increasing this parameter, the investment cost rates and also exergy destruction cost rate of the air compressor and combustion chamber is elevated. Thus, the net effect is a minimum value for the total cost rate.

Figure 9(a) and (b) demonstrate the effects of APH outlet temperature on the system performance. By rising this parameter, the fuel mass rate decreases that leads to a reduction in the input energy and exergy into the system. Also, by reducing the fuel mass flow rate, the temperature of the gas turbine exhaust reduces causing a reduction in the mass flow rate, and consequently, the exergy rate of the obtained steam in the HRSG. These variations lead to a reduction in the energy and exergy efficiencies of the system. Also, fuel and investment cost rates and irreversibility reduce with this parameter. As a results the total cost rate of the system will be reduced with the output temperature of the APH.

According to Figure 10, the energy and exergy efficiencies of the CCHP system improve with the combustion chamber outlet temperature. An increase in the combustion chamber outlet temperature reduces the air and fuel mass flow rates, which causes a decrease in the input

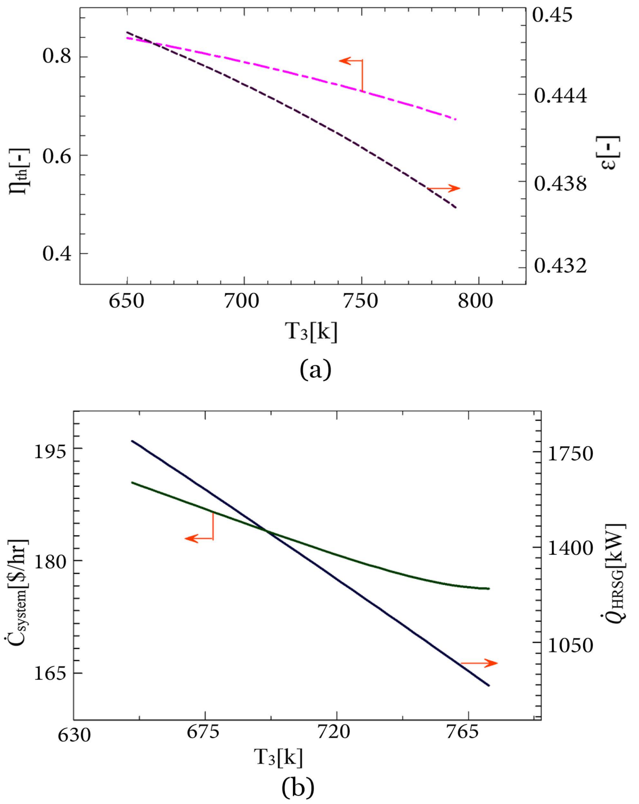

Figure 9. Effects of air preheater outlet temperature on the (a) energy and the exergy efficiencies and (b) heat generated in the HRSG and the total cost rate.

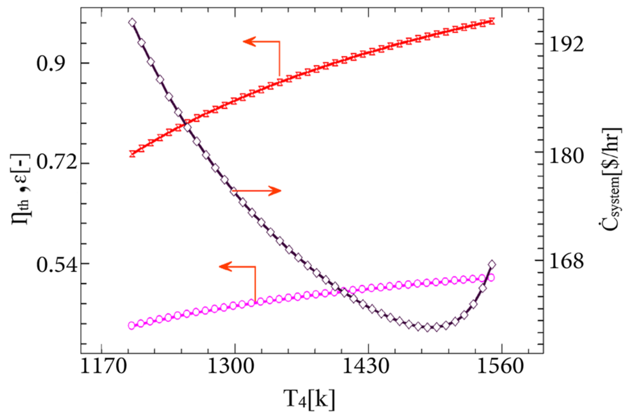

Figure 10. The effect of gas turbine inlet temperature on the energy and exergy efficiencies and the total cost rate of the system.

energy to the CCHP system. But on the other hand, by rising this parameter, temperature of the combustion products at the HRSG inlet, and also, water flow rate of HRSG will rise. As a result, the recovered heat in the HRSG increases that leads to an improvement in the energy and exergy efficiencies.

By reduction of the flue mass flow rate with rising the combustion chamber outlet temperature, the cost rates related to initial investment and the total exergy destruction increase but fuel cost rate reduces. These changes cause a minimum value for the system total cost rate at the higher temperatures.

Figure 11(a) and (b) show the variations of performance parameters with the gas heater outlet temperature. By increasing this parameter, the heat input to the bottoming cycle will certainly decrease, and consequently, the mass flow rate of carbon dioxide, bottoming cycle output power

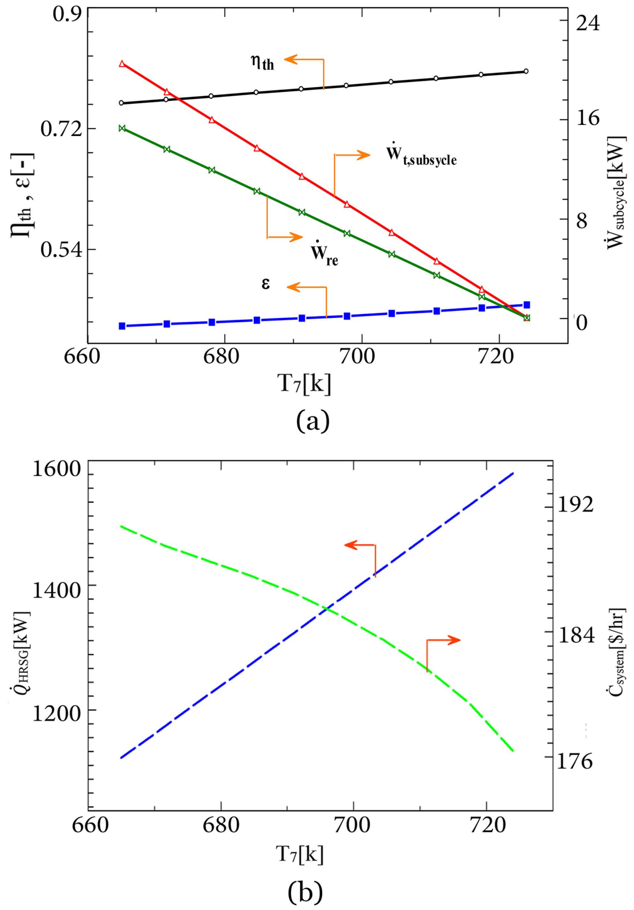

Figure 11. Effects of gas heater outlet temperature on the (a) energy and exergy efficiencies and the bottoming cycle produced power and (b) heat generated in the HRSG and the total cost rate of the system.

and the amount of refrigeration effect will decrease. But on the other side, the amount of produced steam in the HRSG (state 24) increases, which leads to an increase in the amount of obtained energy and exergy. The reduction in the power and refrigeration of the bottom cycle is less than the rise in the steam exergy. Thus, sum of these variations makes a rise in the energy and the exergy efficiencies. Moreover, by reduction of the mass flow rate of working fluid (CO_2), irreversibility and its related cost rate and investment cost rates of the system components reduce. Thus, the total cost rate of the CCHP system decreases by rising of the temperature of the flue gases at the gas heater outlet (state 7).

Figure 12(a) and (b) show the effects of ejector back pressure on the system performance. As can be seen, with increasing this parameter decreases the HP-compressor power due to the reduction in the pressure ratio. Owing to the enhancing HP-compressor inlet pressure and since the HP-compressor outlet pressure is constant, the HP-compressor outlet temperature drops. Considering a constant heat transfer, the temperature difference of the refrigerant in the gas heater increases leading to a reduction in the mass flow rate. With the reduction of the mass flow rate, the transferred heat in the heater and the amount of produced cooling effect by the evaporator will certainly reduce. On the other hand, by reducing the power consumption of the HP-pressure compressor, the net output power of the bottoming cycle

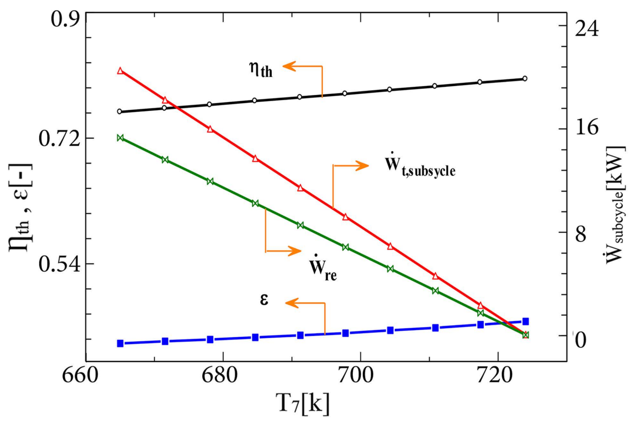

(a)

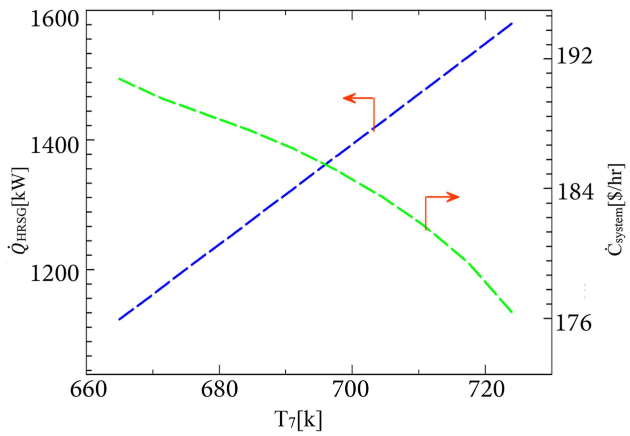

(b)

Figure 12. Effects of ejector back pressure on the (a) energy and exergy efficiencies and (b) refrigeration effect and the total cost rate.

increases. All in all, with rising the ejector back pressure, the energy efficiency decreases while the exergy efficiency increases. Also, with increasing the ejector back pressure, the total exergy destruction rate and investment cost rate of S-CO_2 components including ejector, evaporator, turbines and compressors decrease leading to a reduction in the total cost rate of the system.

The effects of HP turbine inlet temperature on the system performance is depicted in Figure 13(a) and (b). As the inlet temperature of the turbine increases, the temperature difference of the refrigerant in the gas heater cold side rises. Because of the amount of heat transfer is constant, it will reduce the mass flow of refrigerant in the cycle and as a result, the power consumption of the HP compressor and cooling effect in the evaporator decrease. On the other hand, by increasing this parameter, the produced power of HP turbine and the inverted Brayton cycle increases. All in all, these changes will lead to increasing the energy and exergy efficiencies. Also, reduction of the mass flow rate causes a lower exergy destruction and investment cost rates of SCO_2 cycle components and as a result, the total cost rate of the system will reduce.

Figure 14(a) and (b) show the impacts on the system performance of the HP-turbine back pressure. As the turbine back pressure increases, due to the reduction of the pressure ratio, and consequently, decreasing the enthalpy difference in HP-turbine, the produced power by the HP turbine will decrease while the produced power by the LP turbine will increase due to the increasing the pressure ratio.

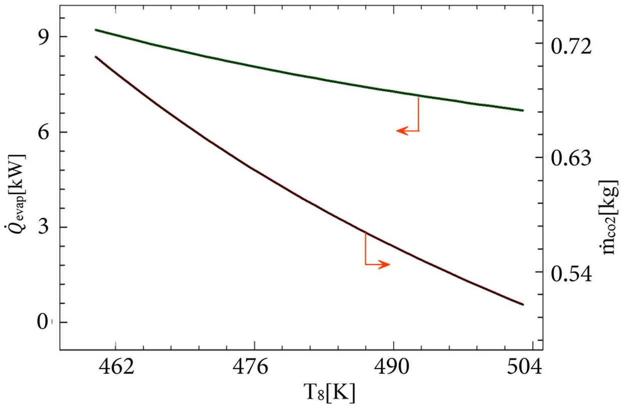

(a)

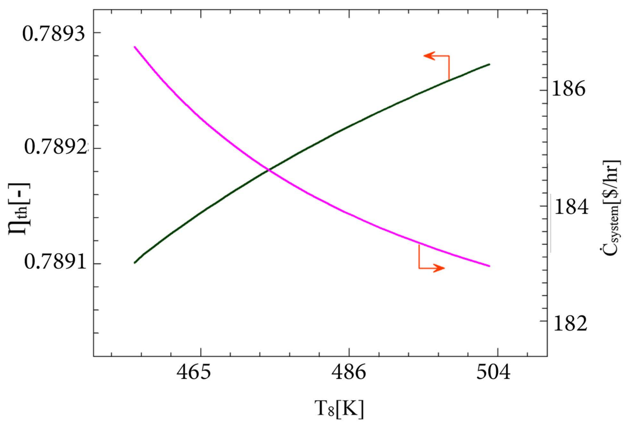

(b)

Figure 13. Effects of high-pressure turbine inlet temperature on the (a) refrigeration effect and mass rate of carbon dioxide and (b) energy efficiency and total cost rate of the system.

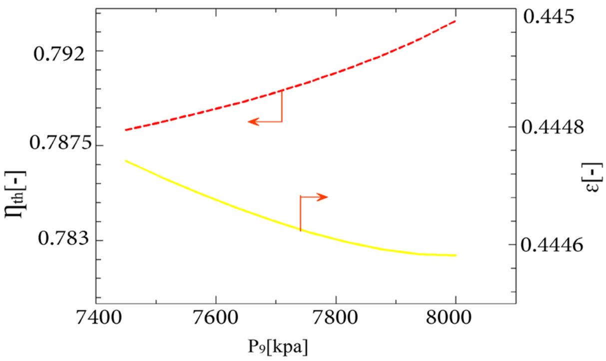

(a)

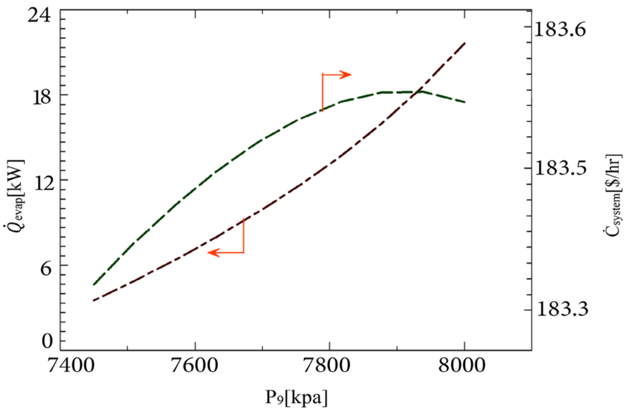

(b)

Figure 14. Effects of HP-turbine back pressure on the (a) energy and the exergy efficiencies (b) refrigeration output in the evaporator and total cost rate of the system.

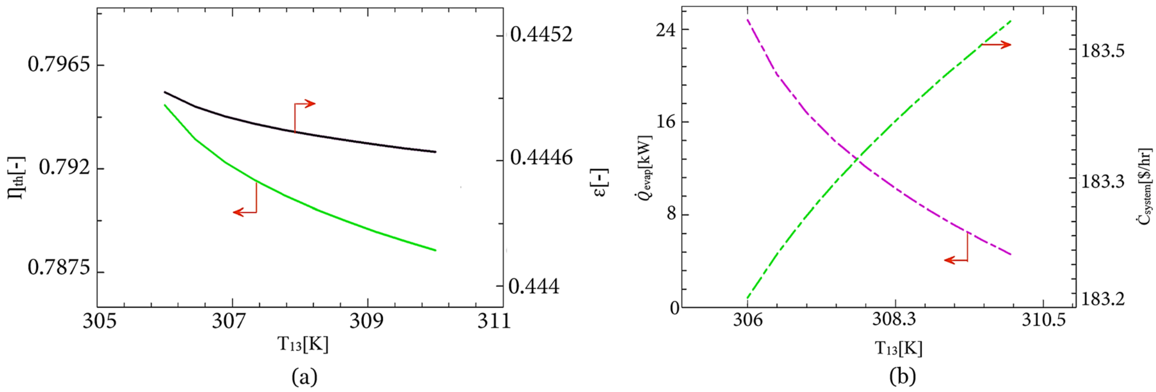

Figure 15. Effects of the ejector inlet temperature on the (a) energy and the exergy efficiencies and (b) refrigeration output in the evaporator and total cost rate of the system.

Also, the amount of heat exchanged in the heater reduces due to the decrease in the heater inlet temperature. On the other hand, the input power of the LP-compressor will increase significantly. With increasing HP turbine back pressure, the pressure of primary input stream to the ejector increases and the velocity of the primary output stream from the nozzle section increases, which leads to an enhancement in the ratio of the secondary to primary mass stream rate in the ejector. Also, the quality of carbon dioxide leaving the ejector decreases, and as a result, the quality of inlet carbon dioxide to the evaporator will decrease causing an increase in the refrigerant enthalpy difference in the evaporator. This leads to an increase in the produced cooling effect by the evaporator. Considering all these changes, by increasing the HP turbine back pressure, the energy efficiency will increase and the exergy efficiency will drop slightly. As P_9 increases, the irreversibility and its associated costs and also investment cost rate increase for the S-CO_2 cycle causing an increase in the total cost of the system.

Figure 15(a) and (b) depict the effects of the ejector inlet temperature on the system performance. As this parameter increases, the quality of the outlet carbon dioxide from the ejector increases, which leads to an increase in the quality of inlet carbon dioxide to the evaporator. Thus, the refrigerant enthalpy difference in the evaporator reduces, and consequently, the amount of the cooling effect decreases which causes a reduction in both thermal and exergy efficiencies of the system. The most important reason for the increase in the system total cost rate is increasing the exergy destruction and its associated costs in the S-CO_2 cycle components.

Figure 16 shows the effects of the turbine back pressure of the inverted Brayton cycle on the output power of the ejector refrigeration sub cycle. As can be seen from this figure, the best amount of pressure to expel carbon dioxide from the LP- turbine is 5300 kPa. If it is lower than 5300 kPa, the input power of the LP-compressor will increase and as a result, the total power will decrease. On the other hand, if it is more than 5300 kPa, it causes carbon dioxide to convert to compressed liquid. Therefore, the output pressure of the LP- turbine should not exceed 5300 kPa.

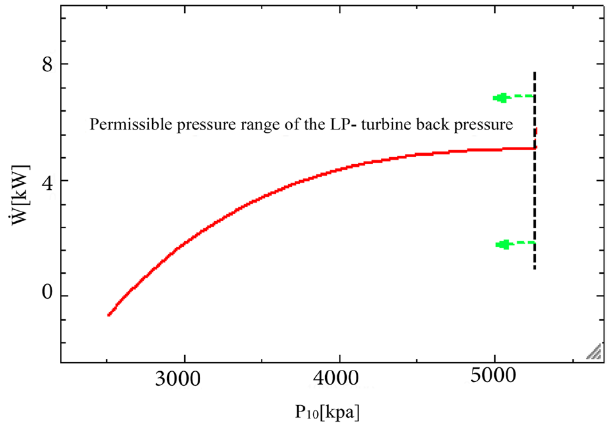

Figure 16. Effects of the turbine back pressure of the inverted Brayton cycle (LP turbine) on the power produced of bottoming cycle.

6. Conclusions

In the present work, the thermodynamic and exergoeconomic simulation of the proposed novel system was performed. The system is a combination of the gas turbine cycle, Brayton cycle, inverted Brayton cycle and the transcritical carbon dioxide refrigeration cycle with ejector-expansion. The most important results of the study can be summarized as:

- The highest exergy destruction rate occurs in the combustion chamber, heat recovery steam generator and gas turbine, respectively;
- By applying the inverted Brayton cycle, the total power of the ejector refrigeration cycle will be positive, and the best possible amount of back pressure of the inverted Brayton cycle turbine (LP- turbine) will be 5300 kPa, which leads to a production power of 5 kW in the bottoming cycle;
- The energy and exergy efficiencies will improve by 48.9% and 54%, respectively, compared to the gas turbine cycle, and also efficiencies of this proposed system will increase by 49.0% and 57%, respectively, compared to the basic cycle;
- The total cost rate of the system and cost of produced electricity are calculated as 183 \$/h and 52.84 \$/MWh, respectively;
- Increasing the inlet temperature to the turbine and gas turbine will be beneficial for the CCHP system in terms of exergo-economics and thermodynamics;

- Increasing the inlet temperature to the ejector and air preheater outlet temperature causes a reduction in the system performance while results in a maximum value for the total cost rate;
- A rising in the air compressor pressure ratio causes a minimum value for the energy efficiency and a maximum value for the exergy efficiency while the total cost rate increases with this parameter.

Finally, it should be noted that, based-on the results, some parameters have opposite effects on the thermodynamic and economic performances of the system so that increasing one parameter improves the thermodynamic performance of the system, but increases the total cost rate. This trend is sometimes even seen in thermodynamic parameters. In such cases, the designer must make a decision according to the existing needs. In some cases, it may be inevitable to increase the costs to meet the expectations from the system. Moreover, changing some parameters may improve the thermodynamic and economic parameters, but it is not technically possible. In these cases, the designer can give priority to the technical issues.

Nomenclature

BL	Life time (year)
c_F	Average costs associated with fuel ($/GJ)
c_p	Average costs associated with product ($/GJ)
$\dot{C}_D$	Cost rate of exergy destruction ($/h)
$\dot{C}_{Loss}$	Cost rate of exergy loss ($/h)
$\dot{E}$	Exergy rate (kJ/s)
$\dot{E}_D$	Exergy destruction rate (kJ/s)
f	Exergo-economic factor (%)
h	Specific enthalpy (kJ/kg)
$\dot{m}$	Mass flow rate (kg/s)
M	Molecular mass (kg/kmol)
r	Relative cost difference (%)
T	Temperature (K)
$\dot{Z}$	Capital cost rate ($/h)

Greek symbols

ε	Exergy efficiency
η	Efficiency
η_{GT}	Gas turbine isentropic efficiency
η_{AC}	Air compressor isentropic efficiency
η_T	Turbine isentropic efficiency
φ	Maintenance factor

Subscripts and superscripts

0,1, 2, 3 …	Cycle locations
AC	Air Compressor
APH	Air Pre-Heater
CC	Combustion Chamber
CRF	Capital Recovery Factor
D	Destruction
e	Exit condition
Evap	Evaporator
Fuel	Fuel
GT	Gas Turbine
h	Hour
HX	Heat exchanger
HRSG	Heat Recovery Steam Generator
HP	High Pressure
i	Interest rate or inlet condition
k	Component
LP	Low Pressure
R_p	Compressor pressure ratio
Tur	Turbine

Funding

This research did not receive any specific grant from funding agencies in the public, commercial, or not-forprofit sectors.

Conflicts of interest

The authors declare that they have no known competing financial interests or personal relationships that could have appeared to influence the work reported in this paper.

Authors contribution statement

Ali Akbar Darabadi Zare: Writing – original draft; Visualization; Validation; Software; Methodology; Investigation; Formal analysis; Data curation; Conceptualization.

Farzad Mohammadkhani: Writing – original draft; Supervision; Formal analysis.

Mortaza Yari: Writing – original draft; Validation; Supervision; Methodology; Conceptualization.

References

1. Khaljani, M., Saray, R.K., and Bahlouli, K. “Comprehensive analysis of energy, exergy and exergo-economic of cogeneration of heat and power in a combined gas turbine and organic Rankine cycle”, *Energy Conversion and Management*, **97**, pp. 154-165 (2015). https://doi.org/10.1016/j.enconman.2015.02.067

2. Darabadi Zareh, A., Saray, R.K., Mirmasoumi, S., et al. “Extensive thermodynamic and economic analysis of the cogeneration of heat and power system fueled by the blend of natural gas and biogas”, *Energy Conversion and Management*, **164**, pp. 329-343 (2018). https://doi.org/10.1016/j.enconman.2018.03.003

3. Shu, G., Shi, L., Tian, H., et al. “An improved CO_2-based transcritical Rankine cycle (CTRC) used for engine waste heat recovery”, *Applied Energy*, **176**, pp. 171-182 (2016). https://doi.org/10.1016/j.apenergy.2016.05.053

4. Macián, V., Serrano, J.R., Dolz., V., et al. “Methodology to design a bottoming Rankine cycle, as a waste energy recovering system in vehicles. Study in a HDD engine”, *Applied Energy*, **104**, pp. 758-771 (2013). https://doi.org/10.1016/j.apenergy.2012.11.075

5. Yang, K., Zhu, N., Ding, Y., et al. “Thermoeconomic analysis of an integrated combined cooling heating and power system with biomass gasification”, *Energy Conversion and Management*, **171**, pp. 671-682 (2018). https://doi.org/10.1016/j.enconman.2018.05.089

6. Uris, M., Linares, J.I., and Arenas, E. "Feasibility assessment of an Organic Rankine Cycle (ORC) cogeneration plant (CHP/CCHP) fueled by biomass for a district network in mainland Spain", *Energy*, **133**, pp. 969-985 (2017). https://doi.org/10.1016/j.energy.2017.05.160

7. Leonzio, G. "An innovative trigeneration system using biogas as renewable energy", *Chinese Journal of Chemical Engineering*, **26**(5), pp. 1179-1191 (2018). https://doi.org/10.1016/j.cjche.2017.11.006

8. Mohammadi, K. and Powell, K. "Thermodynamic and economic analysis of different cogeneration and trigeneration systems based on carbon dioxide vapor compression refrigeration systems", *Applied Thermal Engineering*, **164**, p. 114503 (2020). https://doi.org/10.1016/j.applthermaleng.2019.114503

9. Persichilli, M., Held, T., Hostler, S., et al. "Transforming waste heat to power through development of a CO_2-based-power cycle", *Energy Conversion and Management X*, **10**, p. 12 (2011). https://doi.org/10.1016/j.ecmx.2022.100212

10. Yari, M. "Performance analysis and optimization of a new two-stage ejector-expansion transcritical CO_2 refrigeration cycle", *International Journal of Thermal Sciences*, **48**(10), pp. 1997-2005 (2009). https://doi.org/10.1016/j.ijthermalsci.2009.01.013

11. Domanski, P.A. "Minimizing throttling losses in the refrigeration cycle", *International Conference of Refrigeration, 19th Proceedings* (1997). https://doi.org/10.1016/j.cjche.2017.11.006

12. Liu, F. and Groll, E.A. "Study of ejector efficiencies in refrigeration cycles", *Applied Thermal Engineering*, **52**(2), pp. 360-370 (2013). https://doi.org/10.1016/j.applthermaleng.2012.12.001

13. Dai, Y., Wang, J., and Gao, L. "Exergy analysis, parametric analysis and optimization for a novel combined power and ejector refrigeration cycle", *Applied Thermal Engineering*, **29**(10), pp. 1983-1990 (2009). https://doi.org/10.1016/j.applthermaleng.2008.09.016

14. Gholizadeh, T., Vajdi, M., and Rostamzadeh, H. "A new trigeneration system for power, cooling, and freshwater production driven by a flash-binary geothermal heat source", *Renewable Energy*, **148**, pp. 31-43 (2020). https://doi.org/10.1016/j.renene.2019.11.154

15. Song, J., Wang, Y., Wang, K., et al. "Combined supercritical CO_2 (SCO_2) cycle and organic Rankine cycle (ORC) system for hybrid solar and geothermal power generation: Thermoeconomic assessment of various configurations", *Renewable Energy*, **174**, pp. 1020-1035 (2021). https://doi.org/10.1016/j.renene.2021.04.124

16. Yari, M. "Exergetic analysis of the vapour compression refrigeration cycle using ejector as an expander", *International Journal of Exergy*, **5**(3), pp. 326-340 (2008). https://doi.org/10.1504/IJEX.2008.018114

17. Tashtoush, B., Megdouli, K., Elakhdar, M., et al. "A comprehensive energy and exergoeconomic analysis of a novel transcritical refrigeration cycle", *Processes*, **8**(7), p. 758 (2020). https://doi.org/10.1016/j.ijrefrig.2020.05.006

18. Wang, Y., Chen, T., Liang, Y., et al. "A novel cooling and power cycle based on the absorption power cycle and booster-assisted ejector refrigeration cycle driven by a low-grade heat source: Energy, exergy and exergoeconomic analysis", *Energy Conversion and Management*, **204**, 112321 (2020). https://doi.org/10.1016/j.enconman.2019.112321

19. Karim, S.H.T., Tofiq, T.A., Shariati, M., et al. "4E analyses and multi-objective optimization of a solar-based combined cooling, heating, and power system for residential applications", *Energy Reports*, **7**, pp. 1780-1797 (2021). https://doi.org/10.1016/j.egyr.2021.03.020

20. Sahu, A.K., Agrawal, N., and Nanda, P. "A parametric study of transcritical CO_2 simple cooling cycle and combined power cycle", *International Journal of Low-Carbon Technologies*, **12**(4), pp. 383-391 (2017). https://doi.org/10.1093/ijlct/ctx006

21. Cao, Y., Dhahad, H.A., Hussen, H.M., et al. "Proposal and evaluation of two innovative combined gas turbine and ejector refrigeration cycles fueled by biogas: Thermodynamic and optimization analysis", *Renewable Energy*, **181**, pp. 749-764 (2022). https://doi.org/10.1016/j.renene.2021.09.043

22. Chen, Y., Lundqvist, P., and Platell, P. "Theoretical research of carbon dioxide power cycle application in automobile industry to reduce vehicle's fuel consumption", *Applied Thermal Engineering*, **25**(14-15), pp. 2041-2053 (2005). https://doi.org/10.1016/j.applthermaleng.2005.02.001

23. Wang, J., Zhao, P., Niu, X., et al. "Parametric analysis of a new combined cooling, heating and power system with transcritical CO_2 driven by solar energy", *Applied Energy*, **94**, pp. 58-64 (2012). https://doi.org/10.1016/j.apenergy.2012.01.007

24. Sinha, A.A., Choudhary, T., Ansari, M.Z., et al. "Energy, exergy, and sustainability a novel comparison of conventional gas turbine with fuel cell integrated hybrid power cycle", *International Journal of Hydrogen Energy*, **47**(80), pp. 34257-34272 (2022). https://doi.org/10.1016/j.ijhydene.2022.07.268

25. Kumar, P., Choudhary, T., and Ansari, M. "Thermodynamic assessment of a novel SOFC and intercooled GT integration with ORC: Energy and exergy analysis", *Thermal Science and Engineering Progress*, **34**, 101411 (2022). https://doi.org/10.1016/j.tsep.2022.101411

26. Mohammadi, A., Kasaeian, A., Pourfayaz, F., et al. "Thermodynamic analysis of a combined gas turbine,

Table A.3. Thermodynamic properties of the state points.

State no.	Working fluid	T (K)	P (kPa)	$\dot{m}$ (kg/s)	$\bar{h}$ (kmol/kJ)	$\bar{s}$ (kmol/kJ)
1	Air	290	101.3	4.439	-4950	193.4
2	Air	593.9	1013	4.439	4110	195.6
3	Air	700	962.4	4.439	7402	201.1
4	Combustion gases	1250	923.9	4.622	-1728	221.8
5	Combustion gases	820.2	110.9	4.622	-16597	224.9
6	Combustion gases	724.2	110.9	4.622	-19752	220.8
7	Combustion gases	704.8	110.9	4.622	-20383	219.9
8	CO_2	493.2	15000	0.5478	5858	-24.52
9	CO_2	432.6	7600	0.5478	3878	-23.7
10	CO_2	402.7	5300	0.5478	2900	-23.34
11	CO_2	290	5300	0.5478	-4062	-44.1
12	CO_2	316.6	7600	0.5478	-3490	-43.92
13	CO_2	309.2	7600	0.5478	-4757	-47.97
14	CO_2	291.2	5470	0.712	-4465	-45.73
15	CO_2	291.2	5470	0.02789	-11328	-69.2
16	CO_2	278.2	3969	0.02789	-11368	-68.7
17	CO_2	278.2	3969	0.1642	-122.7	-47.47
18	CO_2	278.2	3969	0.1642	-3490	-40.61
19	CO_2	278.2	3969	0.1363	-4185	-43.11
20	CO_2	291.2	5470	0.6841	-4185	-44.67
21	CO_2	291.2	5470	0.1363	-4185	-44.67
22	CO_2	291.2	5470	0.5478	-4185	-44.67
23	CO_2	369.3	15000	0.5478	-2342	-43.992
24	Combustion gases	422.7	110.9	4.622	-29229	204

ORC cycle and absorption refrigeration for a CCHP system", *Applied Thermal Engineering*, **111**, pp. 397-406 (2017).https://doi.org/10.1016/j.applthermaleng.2016.09.098

27. Zare, A.D., Saray, R.K., and Mirmasoumi, S. "Optimization strategies for mixing ratio of biogas and natural gas co-firing in a cogeneration of heat and power cycle", *Energy*, **181**, pp. 635-644 (2019). https://doi.org/10.1016/j.energy.2019.05.182.

28. Bejan, A., Tsatsaronis, G., and Moran, M.J., *Thermal Design and Optimization*, John Wiley and Sons (1995). https://doi.org/10.1016/j.enconman.2023.116752

29. Zare, A.A.D., Yari, M., Nami, H., et al. "Low-carbon hydrogen, power and heat production based on steam methane reforming and chemical looping combustion", *Energy Conversion and Management*, **279**, p. 116752 (2023). https://doi.org/10.1016/j.enconman.2023.116752

30. Gholizadeh, T., Vajdi, M., and Rostamzadeh, H. "Energy and exergy evaluation of a new bi-evaporator electricity/cooling cogeneration system fueled by biogas", *Journal of Cleaner Production*, **233**, pp. 1494-1509 (2019). https://doi.org/10.1016/j.jclepro.2019.06.086

Appendix A

Several supplementary tables |(Tables A.1-A.3) have been provided in the Appendix to offer additional clarification and support for the main findings of the manuscript. These tables present detailed data and analyses that complement the results discussed in the main text, allowing readers to gain a more comprehensive understanding of the study.

Table A.1. Input parameters of the modeling [27,29,30].

Design parameters	Value
P_0 (kPa)	101.3
T_0 (K)	298.15
$\dot{W}_G$ (kW)	1000
η_{AC} (%)	86
η_{GT} (%)	86
Rp_{AC} (−)	8-15
T_3 (K)	650-770
T_4 (K)	1200-1550
T_7 (K)	665-725
P_{14} (kPa)	5000-5800
T_8 (K)	460-505
P_9 (kPa)	7440-8000
P_{10} (kPa)	2500-6500
T_{13}(K)	305-313

Table A.2. Investment cost for the components [2,29].

Component	Purchased equipment cost
Air pre-heater	$pec_{APH} = 4122 \times (\frac{\dot{m}_g \times \Delta h_{APH}}{u \times \Delta T_{Lm,APH}})^{0.6}$
Air compressor	$pec_{AC} = (\frac{71.10\dot{m}_{air}}{0.9 - \eta_{is,c}})(\frac{P_{out}}{P_{in}})\, ln(\frac{P_{out}}{P_{in}})$
Heat Recovery Steam Generator (HRSG)	$pec_{HRSG} = 6570 \times [(\frac{\dot{Q}_{ec}}{\Delta T_{lm,ec}})^{0.8}$ $+(\frac{\dot{Q}_{ev}}{\Delta T_{lm,ev}})^{0.8}] + 21276 \times \dot{m}_w + 1184.4 \times \dot{m}_g{}^{1.2}$
Combustion chamber	$pec_{CC} = \frac{46.08 \times \dot{m}_{air}}{0.995 - \frac{P_4}{P_3}}[+ exp(0.018T_4 - 26.4)]$
Gas turbine	$pec_{GT} = \frac{479.34 \times \dot{m}_g}{0.92 - \eta_{GT}} ln(\frac{P_4}{P_5}) \times [1$ $+ exp(0.036T_4 - 54.4)]$
Gas heater	$pec_{gas\ heater} = 1.3 \times (190 + 31 * A_{HE}]$
Evaporator	$pec_{evap} = 6000 \times (\frac{A_{evap}}{100})^{0.7}$
Gas cooler	$pec_{Gas\ cooler} = 130 \times (\frac{A_{Gas\ cooler}}{0.093})^{0.78}$

Biographies

Ali Akbar Darabadi Zare is a doctoral student at the University of Tabriz in Iran, specializing in Mechanical Engineering with a focus on Energy Conversion. With a strong background and passion for energy systems, his research revolves around investigating and advancing the field of energy systems. He has made significant contributions by publishing numerous research papers in top-tier international journals in the domain. Through his research, he aims to contribute to sustainable energy solutions and promote the understanding of efficient energy conversion.

Farzad Mohammadkhani has conducted extensive research in the fields of energy, exergy, environmental analysis of systems, and optimization. Serving as an Assistant Professor at the Engineering Faculty of Khoy, Urmia University, he has made notable contributions through the publication of numerous research papers in esteemed international journals within this domain.

Mortaza Yari has conducted a multitude of research studies focusing on energy, exergy, and environmental analysis of systems and optimization. As a distinguished Professor within the Mechanical Engineering Department at the University of Tabriz, his contributions to the field have been significant. He has been the recipient of numerous prestigious awards in recognition of his substantial scientific services.